Eurasia Journal of Science and Technology
Print ISSN: 2663-1024
Online ISSN: 2663-1016
DOI: https://doi.org/10.61784/ejst3173

BOLT PRETENSION CONVERSION AND SAFETY BOUNDARIES BASED ON EXPERIMENTAL FITTING AND MULTICRITERIA MECHANICAL CONSTRAINTS

Lang Liu, QiFeng Wu, ZhiXin Deng*, XinYue Hu, JianJun Liu, ZhengJie Yang
College of Electromechanical and Vehicle Engineering, Southwest Jiaotong University Hope College, Chengdu 610400, Sichuan, China.
**Corresponding Author: ZhiXin Deng*

Abstract: Rock bolts stabilise mine roadways and underground openings by applying axial prestress, but installation is usually controlled by torque, an indirect proxy for bolt preload. Thread and bearing-surface friction, initial contact seating, bolt diameter, and surrounding rock conditions can change the torque–preload relationship, so the same wrench setting may not deliver consistent support force. This paper determines a least-squares fit for the torque coefficients of 18 mm, 20 mm and 22 mm bolts; then, it identifies when stable conversion occurs using sliding-window variation and correlation criteria. It further evaluates steel-strip effects and a safety envelope bounded by bolt yield, anchorage bond, plate indentation, and installation eccentricity, maps this envelope to the Protodyakonov strength factor, and fitted R-squared values range from 0.9664 to 0.9943; mean transition torques are 115 N m for rock and 140 N m for coal. The steel-strip comparison shows an increase in efficiency of about 15%. For the two cases specified above, indentation indices are 0.0805 and 0.3786, respectively; both are less than one, so no steel strip is needed to prevent indentation at these parameters. With an increase in eccentricity from 0 to 15 mm, the calculated permissible torque drops from 405.05 N·m to 50.69 N·m. Integrated Treatment links measured torque conversion with mechanical safety limits for pretension selection and installation alignment.
Keywords: Rock bolt; Pretension torque; Least-squares calibration; Sliding-window transition; Eccentricity; Safety boundary

1 INTRODUCTION

Rock bolts are often used to stabilise mine roadways and underground openings by applying axial prestress to mobilise the surrounding rock. Torque is generally applied during installation, and thus, the support system is subject to a certain preload. Thread and bearing-surface friction, contact seating, component geometry, and rock deformation make the torque-to-preload relationship variable; thus, the same wrench setting may not produce the same support in different bolt sizes or ground conditions. Recent studies have developed mechanism-based and data-fusion predictions of torque-dependent preload and quantified pretightening-force loss in soft-rock roadways [1-2]. Research on cable-bolt pretension and installation pressure has further shown that anchorage response depends on geological and interface conditions [3-4]. The Load Path is no longer through the steel bar. Bearing plates transmit the bolt force to the rock, and their shape affects load capacity [5]. Rock bolts are subjected to combined static and dynamic loads, prestress relaxation, and time-dependent changes during operation [6-8]. Installation Deviations such as eccentricity and inclination change the load transfer and capacity [9-10]. Therefore, the above research provides a basis for linked assessment of torque conversion, stable-load transition, component-level failure limits and installation tolerances. This paper presents test records of 18 mm, 20 mm and 22 mm bolts under repeated measurements in rock and coal environments, comparisons with and without steel strips, and parameterised mechanical cases. Least-squares regression estimates diameter-specific torque coefficients and fit quality. A sliding-window method is used to combine local variation and correlation criteria for identifying when the early compaction response has become sufficiently stable. The steel-strip evaluation compares fitted coefficients and determines the limits of bolt-yield, anchorage-bond and plate-indentation. An eccentric-load model combines axial tension, bending and torsion under a von Mises criterion to correct the local plate-pressure estimate. Finally, a parameter study maps the Protodyakonov strength factor to a safe-torque envelope using the specified safety multiplier. Thus, observed transition statistics differ from calculated capacity limits; the former are based on repeated tests, while the latter depend on the selected bolt, anchorage, plate and rock parameters. Compare the two sets of geological parameters with and without steel strips, evaluate five eccentricities, and report six strength-factor cases. Torque settings are therefore context-specific indicators rather than universal force guarantees; the reported limits only apply to the listed parameter cases. Thus, it will guide the analysis. Based on whether the test-derived statistics are parameter-independent or not, a feasible pretension and its corresponding installation alignment for the support structure can be chosen reasonably.

2 EXPERIMENTAL DATA AND CONVERSION MODEL

2.1 Torque-to-Preload Calibration

© By the Author(s) 2026, under the CC BY-NC-ND license (http://creativecommons.org/licenses/by-nc-nd/4.0).

Experimental records include nominal bolt diameters of 18, 20 and 22 mm. The elastic transfer range applies a torque that is related to the axial preload by a diameter-dependent torque coefficient. Measured points do not pass through the origin exactly; therefore, a fitted model includes an intercept to account for initial friction, system zero drift, elastic seating and assembly variation.

$$T = K \cdot P \cdot d \tag{1}$$

$$P = \alpha \cdot T + b \tag{2}$$

$$\hat{\alpha} = \frac{\sum_{i=1}^{n}(T_i - \bar{T})(P_i - \bar{P})}{\sum_{i=1}^{n}(T_i - \bar{T})^2} \tag{3}$$

$$\hat{b} = \bar{P} - \hat{\alpha}\bar{T}; \quad K = 1/(\hat{\alpha} d) \tag{4}$$

$$R^2 = 1 - Q/SST \tag{5}$$

The fitted slopes, intercepts, torque coefficients and determination coefficients are listed in Table 1. All reported determination coefficients are greater than 0.96, indicating strong linearity of the measurement range. The diameter-dependent fitted slopes and measured points are shown in Figure 1.

Table 1 Least-Squares Calibration of Torque and Preload by Bolt Diameter

Diameter (mm)	Slope α	Intercept b	Torque coefficient K	R^2
18.0	0.3287	2.9843	0.1690	0.9664
20.0	0.2703	0.5257	0.1850	0.9874
22.0	0.2425	−0.8414	0.1875	0.9943

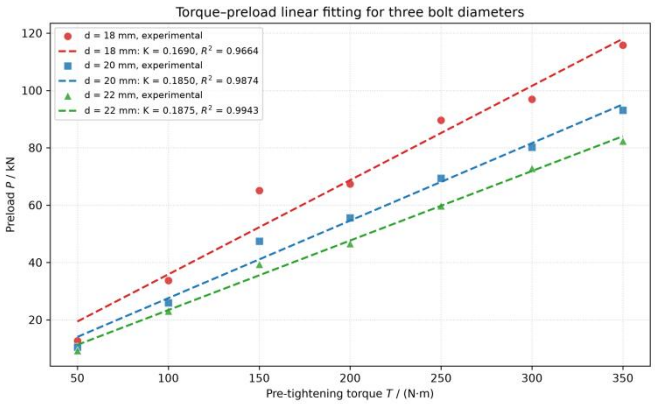

Figure 1 Torque-Preload Regression Lines for the Three Bolt Diameters

2.2 Identifying the Transition to Stable Transfer

First, there is a brief contact-compaction stage; afterwards, a relatively stable linear transfer period begins. Five repeated preload readings are available for each torque level. A sliding window calculates the coefficient of variation to assess local dispersion and uses the correlation coefficient for local linearity. The thresholds for analysis are set at 0.35 and 0.99, respectively, and the first torque level that meets both criteria is chosen as the transition point.

$$T_{crit} = \min\{T_k : r_k \geq 0.99,\ CV_k \leq 0.35\} \tag{6}$$

Table 2 shows the five detected thresholds under each condition: the rock mean is 115 N·m (SD 13.69), coal averages 140 N·m (SD 85.88), and spans 75-275 N·m. The two transition patterns are compared directly in Figure 2, and although the means are relatively close, the spread of the coal measurements is much greater.

Table 2 Sliding-Window Transition Torque Results for Rock and Coal Conditions

Condition	Five replicate transition torques (N·m)	Mean (N·m)	SD (N·m)
Rock	125, 100, 100, 125, 125	115	13.69
Coal	75, 175, 275, 100, 75	140	85.88

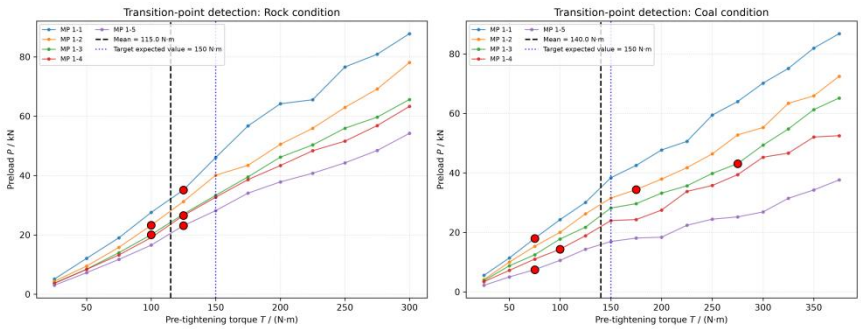

Figure 2 Transition-Point Detections under Rock and Coal Conditions

3 MECHANICAL SAFETY AND DESIGN BOUNDARIES

3.1 Steel-Strip Efficiency and Component Limits

A steel strip is added to modify the contact stack and spread the bearing pressure over a wider area. Fitted coefficients with and without the strip are compared to determine the relative conversion gain from the coefficient reduction. Table 3 lists the fitted coefficients and corresponding conversion gains.

$$G = (Kbase - Kstrip)/Kbase \times 100\% \quad (7)$$

Table 3 Fitted Torque Coefficients and Conversion Gains with a Steel Strip

Diameter (mm)	Baseline K	With strip K	Gain (%)
18	0.1690	0.1437	14.97
20	0.1850	0.1572	15.03
22	0.1875	0.1593	15.04

The maximum allowable torque is restricted by bolt yielding, anchorage-bond strength and plate-induced rock indentation. The two cases considered are a 20 mm rock bolt with a yield load of 170 kN, a rock modulus of 15 GPa, Poisson's ratio of 0.25, a 150 mm plate, and an allowable indentation of 1.0 mm; and a 22 mm coal bolt with a yield load of 205 kN, a modulus of 2 GPa, Poisson's ratio of 0.35, an 180 mm plate, and an allowable indentation of 1.5 mm. The steel-strip coefficients for these cases are 0.1572 and 0.1593. The obtained torque limits and indentation checks are shown in Table 4.

$$Tsafe = \min\{Tyield, Tbond, Tindent\} \quad (8)$$

Table 4 Computed Torque Limits and Indentation Checks for the Two Parameter Sets

Condition	Tmax (N·m)	Indentation (mm)	Allowable (mm)	Index ξ	Strip required for indentation?
Rock (A)	534.480	0.080492	1.0	0.080492	No
Coal (B)	718.443	0.567827	1.5	0.378551	No

Both indentation indices are less than 1 under the above circumstances; thus, the calculated plate-indentation condition does not require a strip. The strip still lowers the fitted torque coefficient and yields gains of about 15% for all three tested diameters. Figure 3 compares the calculated torque capacities and indentation indices for the two cases.

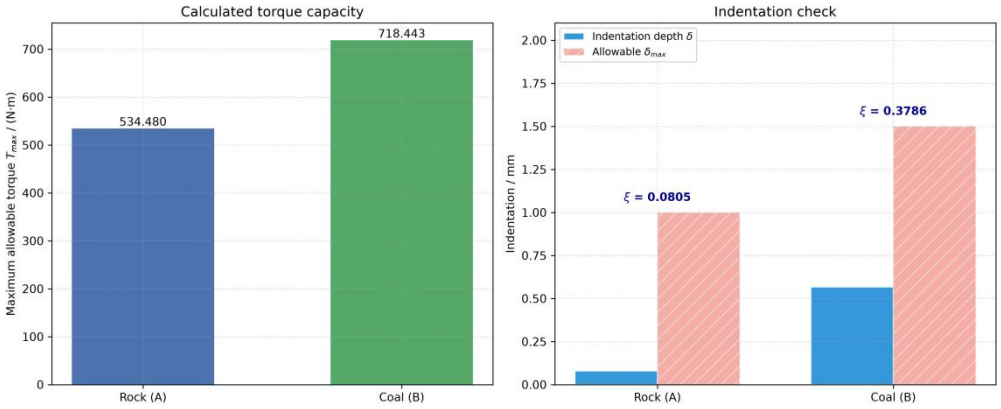

Figure 3 Comparison of Calculated Torque Capacity and Indentation Indices

3.2 Eccentric Loading and Safety Envelope

An installation offset of the bolt axis from the plate centre will cause a bending moment due to axial tension and torsion. The combined stress is determined according to the von Mises criterion, and the local plate pressure is corrected by an eccentricity factor. Table 5 presents the calculated torque limits and sensitivity measures for the tested offsets.

$$M = P \cdot e \quad (9)$$

$$\sigma eq = \sqrt{(\sigma t + \sigma b)^2 + 3\tau^2} \leq [\sigma] \quad (10)$$

$$\beta e = 1 + 6e/a \quad (11)$$

Table 5 Eccentricity Sensitivity of Permissible Torque and Its Derivatives

Eccentricity e (mm)	Tmax (N·m)	Sensitivity (N·m/mm)	Elasticity E(e)
0	405.05	−187.34	−0.0000
2	209.65	−50.51	−0.4835
5	121.47	−16.98	−0.7014
10	71.68	−5.92	−0.8241
15	50.69	−2.96	−0.8757

The permissible torque decreases from 405.05 N·m at zero offset to 50.69 N·m at 15 mm, a reduction of 87.5%. The reported sensitivity is negative, but the absolute elasticity is less than one. Figure 4 shows the sensitivity curve and a relatively steep drop in small offsets.

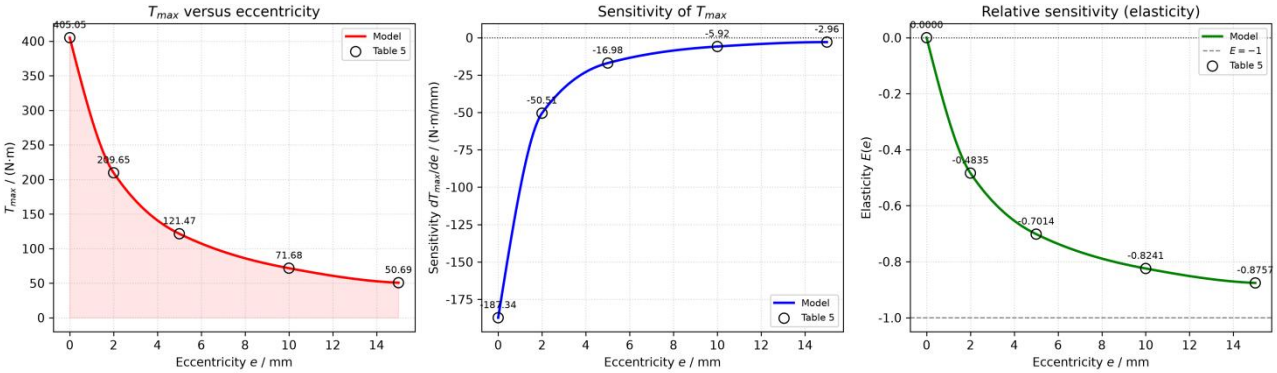

Figure 4 Eccentricity Effects on Permissible Torque, Sensitivity, and Elasticity

3.3 Protodyakonov-Factor Torque Selection

The final model considers a material-strength limit, an anchorage limit that rises with the Protodyakonov factor, and a plate-indentation limit related to rock stiffness. Apply a safety factor of 0.8 to the lower bound of active constraint; Table 6 shows the resulting limits and safety-corrected recommendations for different Protodyakonov factors.

$$\mathrm{Topt(f)} = 0.8 \cdot \min\{\mathrm{Tmaterial},\ \mathrm{Tanchor(f)},\ \mathrm{Tplate(f)}\} \tag{12}$$

Table 6 Safety-Envelope Calculations across Selected Protodyakonov Factors

f	Bolt-material limit (N·m)	Anchorage limit (N·m)	Indentation limit (N·m)	Recommended torque (N·m)
1	121.845	870.849	432	97.476
2	121.845	1,108.354	864	97.476
3	121.845	1,345.858	1,296	97.476
5	121.845	1,820.867	2,160	97.476
8	121.845	2,533.380	3,456	97.476
10	121.845	3,008.389	4,320	97.476

Among the listed parameters, the material-strength limit is the smallest of the three calculated capacities at all sampled factors, and the recommended value is 97.48 N·m for all. Safety-envelope curves are shown in Figure 5. This numerical result is only for the stated bolt and plate parameters; therefore, the governing boundary is determined by the minimum of the three limits.

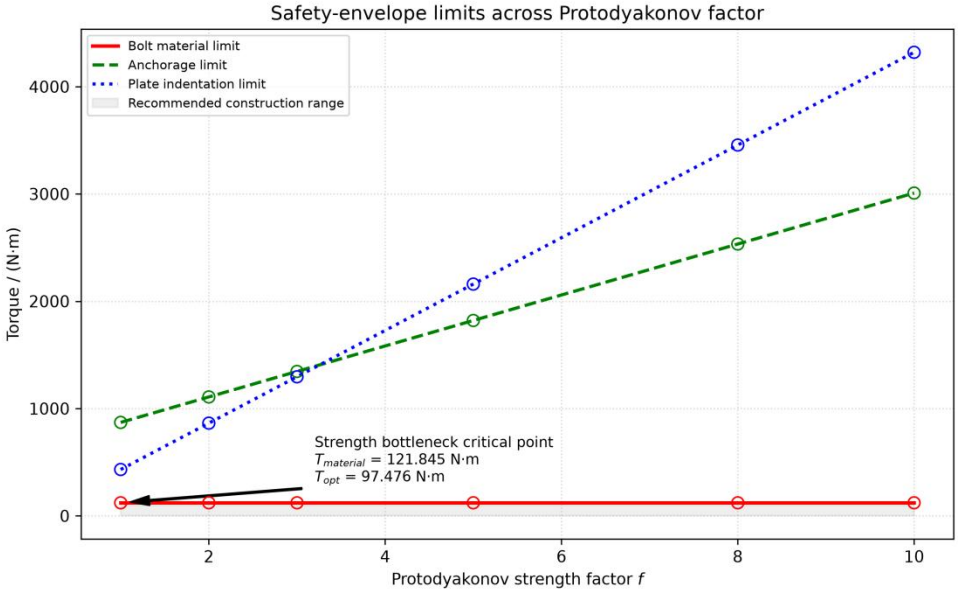

Figure 5 Safety-Envelope Limits across the Protodyakonov Factor

4 CONCLUSION

The test-derived torque coefficient is a relatively small link between installation torque and axial preload, and the sliding-window criteria distinguish early contact compaction from the more stable transfer regime. The 18-22 mm fit results are highly linear; however, the coal transition points are much more scattered than those of the rock. Steel strips reduce the fitted coefficient by approximately 15%, but both modeled indentation indices remain below the stated failure threshold.

Mechanical Safety is not solely determined by the nominal conversion coefficient. Yield, anchorage and plate-indentation limits form a minimum-capacity envelope; eccentricity sharply reduces the allowable torque, especially near zero offset. Under the listed Protodyakonov cases, the material limit governs and the safety-adjusted recommendation is 97.48 N·m. Together, these calculations link the laboratory conversion behaviour with installation alignment and component-level limits for the evaluated support cases. These results support feasibility as a screening method for the tested 18–22 mm bolts and specified support configurations: measured torque-conversion coefficients can be paired with yield, bond, indentation, and eccentricity limits to define a transparent installation envelope. The conclusions remain limited to the tested sizes and parameterized conditions and should not be treated as universal field settings. Future work should validate the envelope through in-situ installation tests across additional bolt sizes and geological conditions, and incorporate measured friction, preload loss, and dynamic loading into torque selection.

COMPETING INTERESTS

The authors have no relevant financial or non-financial interests to disclose.

REFERENCES

[1] Qiao Y, Zhao B, Deng D, et al. Prediction model for nonlinear variation of bolt preload with tightening torque based on mechanism and data fusion. Scientific Reports, 2025, 15(1): 8020.

[2] Yu F, Sun B, Wang Q, et al. Study on pretightening loss effect of bolt support in deep soft rock roadway. Shock and Vibration, 2024, 2024: 3834064.

[3] Li X, Si G, Oh J, et al. Effect of pretension on the performance of cable bolts and its optimisation in underground coal mines with various geological conditions. International Journal of Rock Mechanics and Mining Sciences, 2022, 152: 105076.

[4] Li C C, Aure A, Knox G. Experimental study of the effects of borehole size, borehole roughness, and installation pressure on the pull load capacity of inflatable rockbolts. Rock Mechanics and Rock Engineering, 2023, 56(11): 8415-8431.

[5] Gaurav K, Kumar R, Mandal P K, et al. Evaluation of a novel pyramidal design of rock bolt bearing plate using analytical, experimental, and numerical methods. Engineering Structures, 2023, 297: 116998.

[6] Kang H, Yuan G, Si L, et al. Mechanical behavior and failure mechanisms of rock bolts subjected to static-dynamic loads. International Journal of Mining Science and Technology, 2024, 34(3): 281-288.

[7] Wang Z, Fang S, Zhang C. Deformation characteristics and response factors of rock bolt body in roadway with layered composite roof. Applied Sciences, 2024, 14(15): 6694.

[8] Wu Q, Xiao H, Weng L, et al. Dynamic mechanical responses and cracking resistance effect of prestressed rockbolt subjected to impact loading. International Journal of Rock Mechanics and Mining Sciences, 2025, 195: 106307.

[9] Guan K, Zhu R, Pérez-Rey I, et al. Creep behavior and prestress relaxation mechanism of bolt-reinforced jointed specimen disturbed by dynamic impact. International Journal of Rock Mechanics and Mining Sciences, 2025, 196: 106338.

[10] Jodeiri Shokri B, Mirzaghorbanali A, Nourizadeh H, et al. Impact of installation variations on axial performance of rock bolts: An experimental and numerical study. Geomechanics and Geophysics for Geo-Energy and Geo-Resources, 2026, 12: 48.